(Supporting Information)

Stabilization of graphene quantum dots (GQDs) by encapsulation inside zeolitic imidazolate framework nanocrystals for photoluminescence tuning

Bishnu P. Biswal,[†] Dhanraj B. Shinde,[†] Vijayamohanan K. Pillai[*, †, ‡] and Rahul Banerjee[*, †]

[†]Physical/Materials Chemistry Division, CSIR-National Chemical Laboratory,
Dr. Homi Bhabha Road, Pune-411008 (India).

[‡]CSIR-Central Electrochemical Research Institute,
Karaikudi-630006, Tamil Nadu (India).

E-mail: r.banerjee@ncl.res.in; vk.pillai@ncl.res.in
Fax: + 91-20-25902636; Tel: + 91-20-25902535

Content **Page**

Section 1: Experimental measurements and methods used:

General Remarks: 2-Methylimidazole (2-mIm) was purchased from Loba chemie, $Zn(NO_3)_2.6H_2O$, Methanol, MWCNT (Nanocyl 95% pure), $LiClO_4$ (98%), Propylene carbonate were purchased from Sigma Aldrich Chemicals. All starting materials were used without further purification.

PXRD, TGA, SEM, Raman, HR-TEM, BET measurements, Water adsorption, XPS, FT-IR, UV-DRS and PL Experiments: The powder X-ray diffraction patterns were recorded using PANalytical X'PERT PRO instrument using iron-filtered Cu Kα radiation (λ=1.5406 Å) in the 2θ range of 5°-50° with a step size of 0.02° and a time of 0.3 second per step. Thermogravimetric analysis (TGA) experiments were carried out in the temperature range of 25–900°C on a SDT Q600 TG-DTA analyzer under N_2 atmosphere at a heating rate of 5°C min^{-1}. Transmission Electron Microscopy (TEM) was carried out by a FEI, TECHNAI 300 instrument operated at an accelerating voltage of 300 kV with a resolution of not less than 3-4 nm. SEM images were obtained with a FEI, QUANTA 200 3D Scanning Electron Microscope with tungsten filament as electron source operated at 10 kV. The samples were sputtered with Au (nano-sized film) prior to imaging by a SCD 040 Balzers Union as well as by coating over Si wafers. Fourier transform infrared (FT-IR) spectra were taken on a Bruker Optics ALPHA-E spectrometer with a universal Zn-Se ATR (attenuated total reflection) accessory in the 600-4000 cm^{-1} region or using a Diamond ATR (Golden Gate). All Raman spectroscopy measurements were carried out at room temperature on an HR 800 Raman spectrophotometer (Jobin Yvon HORIBA, France) using monochromatic radiation emitted by a He-Ne laser (632.8 nm), operating at 20 mW. UV-DR spectra were recorded using JASCO V-570 spectrophotometer after dispersing the materials in solid state. Photoluminoscence spectra (PL) collected using Horiba Jobin Yvon Fluorolog 3 spectrophotometer having a 450 W Xenon lamp, which has been used as excitation source. XPS measurements were carried out on a custom-built laboratory version ambient pressure photoelectron spectrometer (Lab-APPES) instrument with VG Scienta R3000HP analyzer. Low-pressure volumetric gas adsorption measurements were performed at 77 K for N_2, maintained by a liquid nitrogen bath, with pressures ranging from 0 to 760 Torr on a Quantachrome, Quadrasorb automatic volumetric instrument. Water adsorption experiments on Quantachrome Autosorb-iQ-MP automatic volumetric instrument, up to P/P_o=0.9 at 293 K. Confocal images were taken using Zeiss LSM 510 Meta Confocal Microscope.

Section 2: Detailed synthesis procedure of GQDs@ZIF-8 composite:

The GQDs were synthesized by using electrochemical method (*Chem. Eur. J*. 2012, **18**, 12522). For the synthesis of GQDs@ZIF-8 composite materials; methanolic solution of 2-methylimidazole (2-mIm) [200 mg, 2.43 mmol] in 10 mL, into that 100 μL (0.4 wt%) of as-synthesized GQDs (in Propylene carbonate), $Zn(NO_3)_2.6H_2O$ [95 mg, 0.3 mmol] in 5 mL of methanol was added drop wise (immediately some white turbid solution results) and left undisturbed for about 24 hours. After the mentioned period, the resulting white precipitate were collected by centrifuge and dried well under vacuum for 6 hours to get (0.4 wt%) GQDs@ZIF-8. In similar way GQDs (0.8 wt%, and 1.2 wt%)@ZIF-8 composites were synthesized. (GQDs@ZIF-8) **FT-IR** (powder, cm^{-1}); 2940 (s), 1720 (m), 1629 (w), 1445 (s), 1256 (m), 1193 (m), 750 (m). **Elemental Analysis** (%): ZIF-8 [$Zn(mIm)_2$] (**Calculated**): C 42.22, H 4.43, N 24.62; (**Found**): C 41.045, H 4.495, N 22.92. (0.4 wt%) GQDs@ZIF-8: C 41.367, H 4.450, N 23.42; (0.8 wt%) GQDs@ZIF-8: C 41.512, H 4.529, N 22.49; (1.2 wt%) GQDs@ZIF-8: C 41.735, H 4.330, N 23.08.

Note: In order to check the correlation between the concentration of precursors with morphology and size of the composite, we did optimization of the encapsulation procedure by using different amount of GQDs (0.4, 0.8 and 1.2 wt %) as well as the ZIF-8 precursors (Ligand to metal molar ratios of 8:1, 8:1.5 and 8:2) to prepare the GQDs@ZIF-8 hybrid material. However, we did not observe any drastic change in the ZIF-8 crystal morphology (spherical) by changing ligand to metal ratio (8:1 and 8:1.5) from the HR-TEM images. Moreover, when used 8:2 molar ratio (ligand to metal) to prepare the composite from the HR-TEM images we observed that, the GQDs are not encapsulated but agglomerated on the surface of the ZIF-8 crystals.

Section 3: Powder X-ray diffraction (PXRD):

Powder X-ray diffraction patterns of as-synthesized GQDs@ZIF-8 composite shows that almost all ZIF-8 characteristic peaks are retain with two humps at around ~25-35° (2θ) and ~45-48° (2θ), which corresponds to the GQDs peaks; also some broadening of peaks observed.

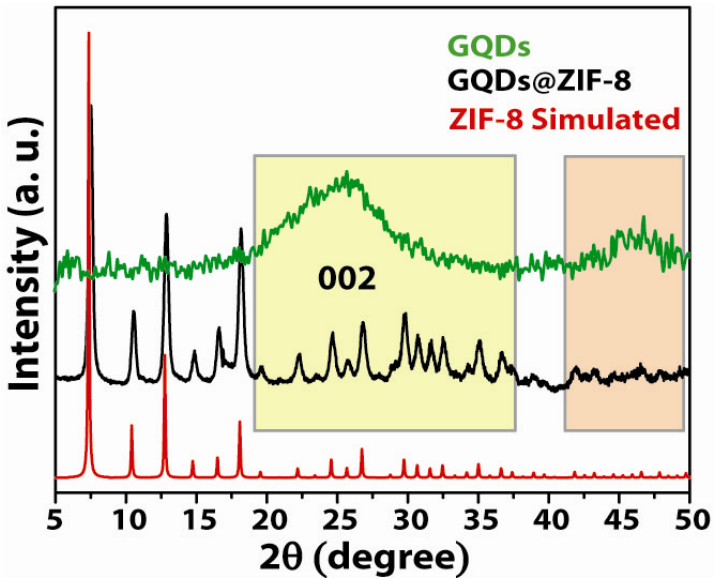

Fig. S1. Simulated and experimental PXRD patterns of ZIF-8, GQDs@ZIF-8 and GQDs. The PXRD paptterns demonstrates the phase purity of (1.2 wt%) GQDs@ZIF-8 in comparison with GQDs and ZIF-8 simulated.

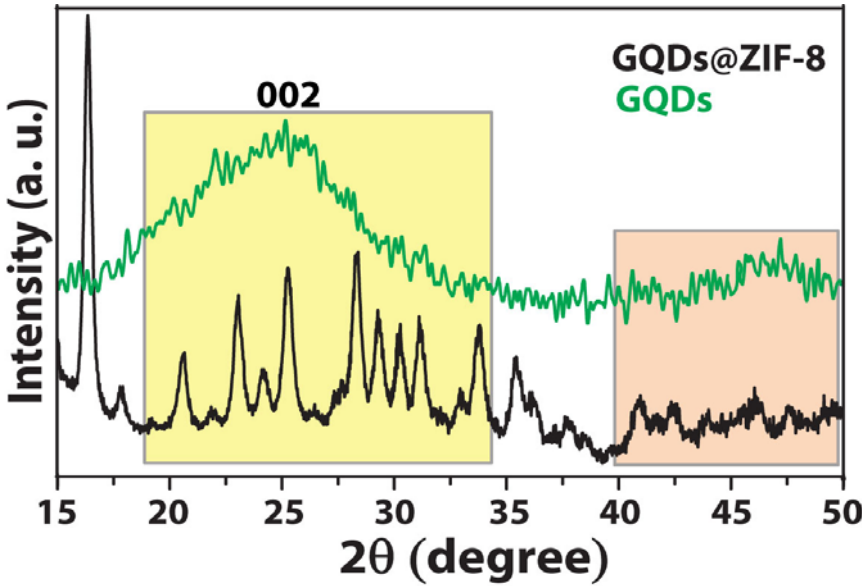

Fig. S2. Zoomed PXRD pattern of GQDs@ZIF-8 in comparison with GQDs showing the brodened peaks at ~25-35° and ~45-48° originating from the GQDs present within the crystals of ZIF-8 in the samples of GQDs@ZIF-8.

Section 4: FT-IR spectra:

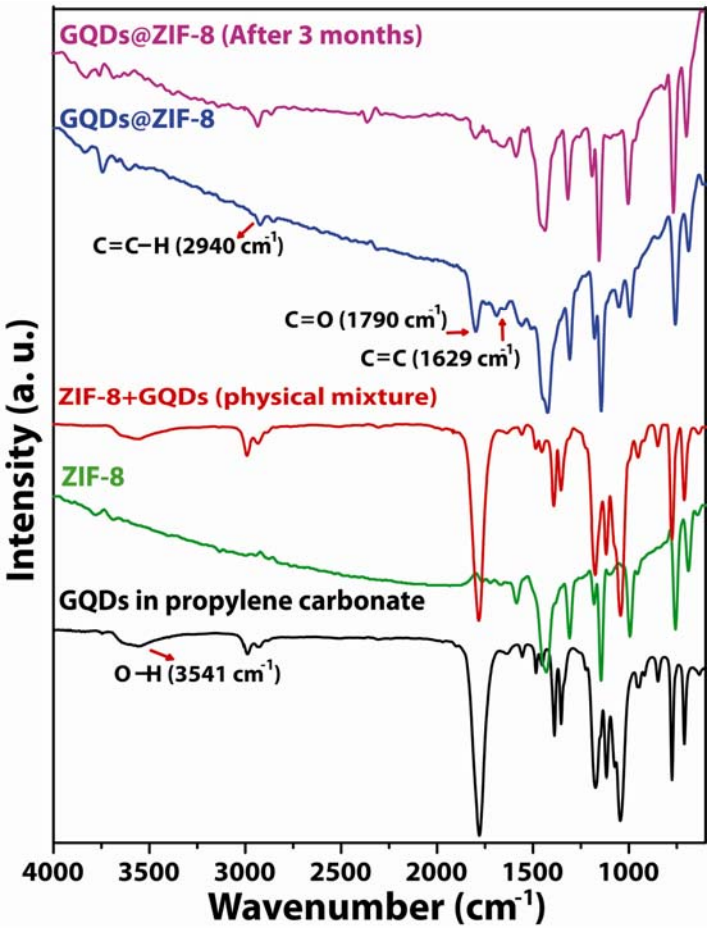

Fig. S3. Smoothened FT-IR spectra of as-synthesized GQDs (black) in comparison with ZIF-8 (green), ZIF-8+GQDs (physical mixture) (red), GQDs@ZIF-8 composite (blue) and GQDs@ZIF-8 composite (pink) after 3 months of synthesis.

Section 5: Thermal stability (TGA):

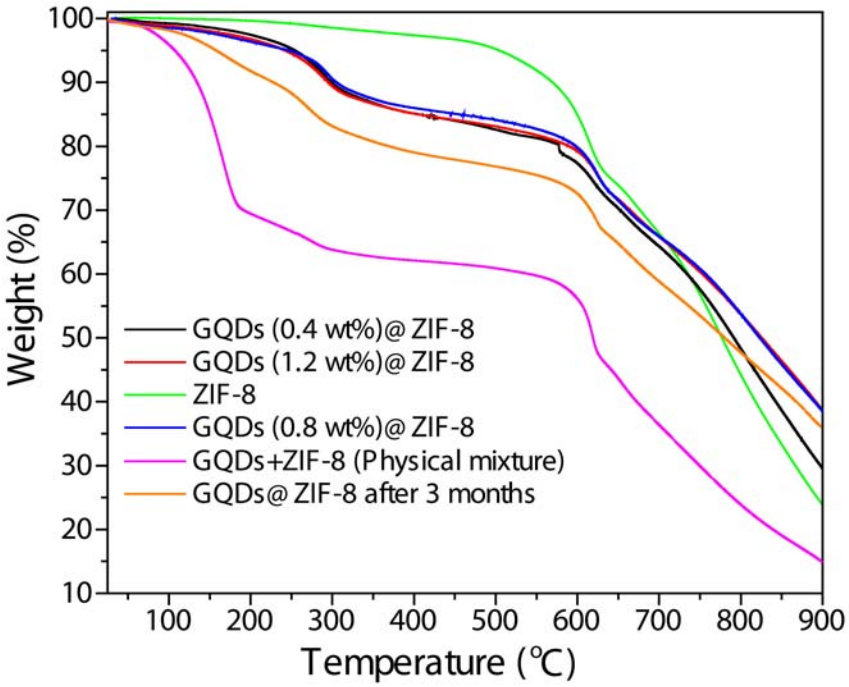

Fig. S4. Thermal gravimetric analysis (TGA) of activated samples of ZIF-8, (0.4 wt%) GQDs@ZIF-8, (0.8 wt%) GQDs@ZIF-8, (1.2 wt%) GQDs@ZIF-8, GQDs+ZIF-8 (physical mixture) and GQDs@ZIF-8 (after 3 months of synthesis) under N_2 atmosphere with 5° ramp rate.

Table S1:

Sample	C	H	N	% Loading From CHN	% Loading From TGA
ZIF-8	41.045	4.495	22.92		
(0.4 wt%) GQDs@ZIF-8	41.367	4.450	23.42	0.35 wt%	0.32 wt%
(0.8 wt%) GQDs@ZIF-8	41.512	4.529	22.49	0.43 wt%	0.51 wt%
(1.2 wt%) GQDs@ZIF-8	41.735	4.330	23.08	0.67 wt%	0.73 wt%

From the TGA profile, we have calculated roughly the amount of GQDs being encapsulated within ZIF-8 crystals (Table S1). For (0.8 wt%) GQDs@ZIF-8 composite, we found ~0.43 wt% weight loss remains at 300 °C; whereas for (1.2 wt%) GQDs@ZIF-8; (~0.67 wt%) in comparison with (0.4 wt%) GQDs@ZIF-8; (~0.35 wt%). These values fairly matches with the values obtained from CHN analysis [(0.4 wt%) GQDs@ZIF-8 composite (~0.32 wt%); (0.8 wt%) GQDs@ZIF-8; ~0.51 wt%; (1.2 wt%) GQDs@ZIF-8, ~0.73 wt% loading of GQDs].

Section 6: Raman analysis:

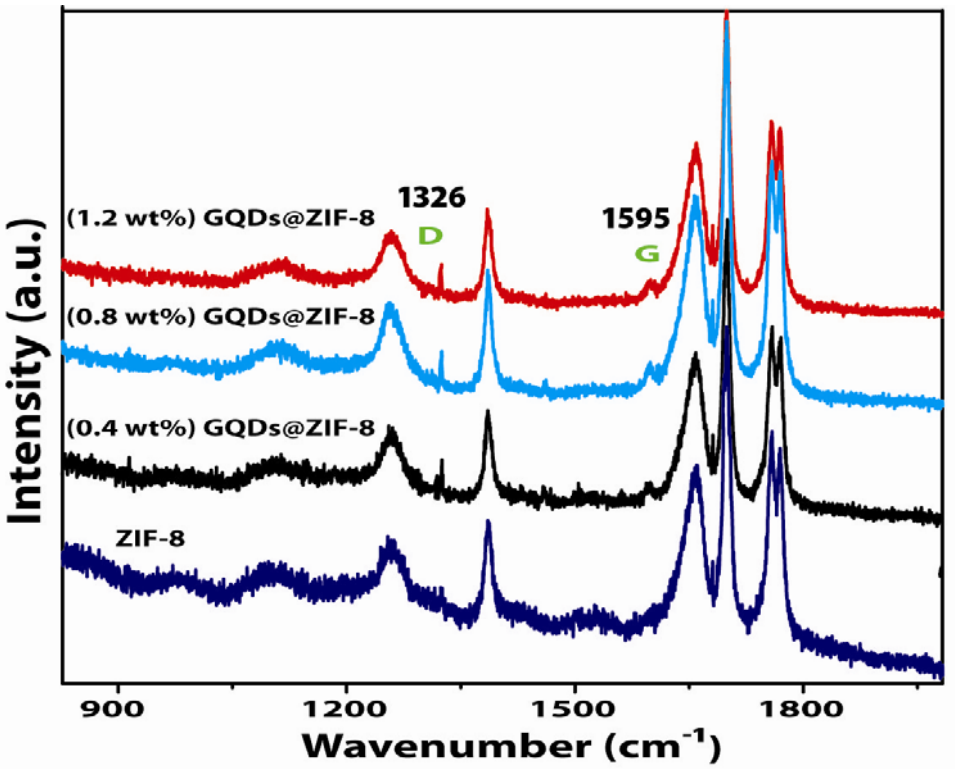

Fig. S5. Raman spectra of different GQDs@ZIF-8 composites in comparison with ZIF-8 showing presence of D (~1326 cm^{-1}) and G band (~1595 cm^{-1}) originating from the GQDs present within the crystals of ZIF-8.

Section 7: N_2 Adsorption analysis (Surface area determination):

Gas Adsorption Measurements: Low-pressure volumetric gas adsorption measurements were performed at 77 K for N_2, maintained by a liquid nitrogen bath, with pressures ranging from 0 to 760 Torr on a Quantachrome, Quadrasorb automatic volumetric instrument. The colourless nano crystals of ZIF-8 and (0.4, 0.8, and 1.2 wt%) GQDs@ZIF-8 were soaked in dried CH_2Cl_2 (DCM):MeOH (v/v 1:1) mixture for 12 h. Dried CH_2Cl_2: MeOH (v/v 1:1) mixture was subsequently added and the crystals were kept for additional 48 h to remove free solvates presented in the framework. The so-obtained material was dried under dynamic vacuum (< 10^{-3} Torr) at RT overnight. The sample were heated under dynamic vacuum at 60 ºC (12 h) to remove the solvent present on the surface and then further heated to 150 ºC (24 h) to remove the non coordinated solvents. Apparent surface areas are 1392, 983, 805, and 673 for ZIF-8, (0.4 wt%) GQDs@ZIF-8, (0.8 wt%) GQDs@ZIF-8, and (1.2 wt%) GQDs@ZIF-8 composites respectively (Brunauer– Emmett–Teller (BET) model [K. S. Walton, R. Q. Snurr, *J. Am. Chem. Soc.* 2007, **129**, 8552] were obtained by using the data points (P/P_o= 0.1-0.3) on the adsorption branch.

From the N_2 adsorption study it reveals that the GQDs are inside the ZIF-8 framework and blocking the pores. For (0.4 wt%) GQDs@ZIF-8 there is a drastic decrease in the surface area which is due to more amount of GQDs are occupying the pore whereas in case of subsequent specimens the surface area decreases, but not to that extend. For the (1.2 wt%) GQDs@ZIF-8 composite the surface area was found to be ~673 m^2g^{-1}. We have also checked the N_2 sorption of the same sample [(1.2 wt%) GQDs@ZIF-8] after 3 months and found that the surface area values was retain (~640 m^2g^{-1}) . However, the physically mixed (ZIF-8+GQDs) showed less surface area (~943 m^2g^{-1}) than the pristine ZIF-8 (1392 m^2g^{-1}), that could be due to the adsorption of solvents into the ZIF-8 pores.

Water Adsorption Measurements of GQDs@ZIF-8 and ZIF-8: Low-pressure volumetric water adsorption measurements were performed at 293 K, with pressure ranging from 0 to 0.9 [relative pressure (P/P_o)] on a Quantachrome Autosorb-iQ-MP automatic volumetric instrument. The colourless nanocrystals of GQDs@ZIF-8 were soaked in dried CH_2Cl_2: MeOH (v/v 1:1) mixture for 12 h. Freshly

dried CH_2Cl_2: MeOH (v/v 1:1) mixture was subsequently exchanged and the crystals were kept for additional 48 h to remove free solvates presented in the framework. The so-obtained material was dried under dynamic vacuum (< 10^{-3} Torr) at RT overnight. The samples were heated under dynamic vacuum at 80 ºC (12 h) to remove the solvent present on the surface and then further heated to 150 ºC (12 h) to remove further solvent molecule floating inside the framework. GQDs@ZIF-8 shows water vapor uptake 34 $cm^3(STP)g^{-1}$, at a relative pressure (P/P_o) of 0.9.

It has been found that, for GQDs@ZIF-8 composite the water vapor uptake is 34 $cm^3(STP)g^{-1}$ at 0.9 (P/P_o) and 293 K, which is almost three fold higher than the water uptake of ZIF-8 [12 $cm^3(STP)g^{-1}$ at 0.9 (P/P_o) and 293 K].

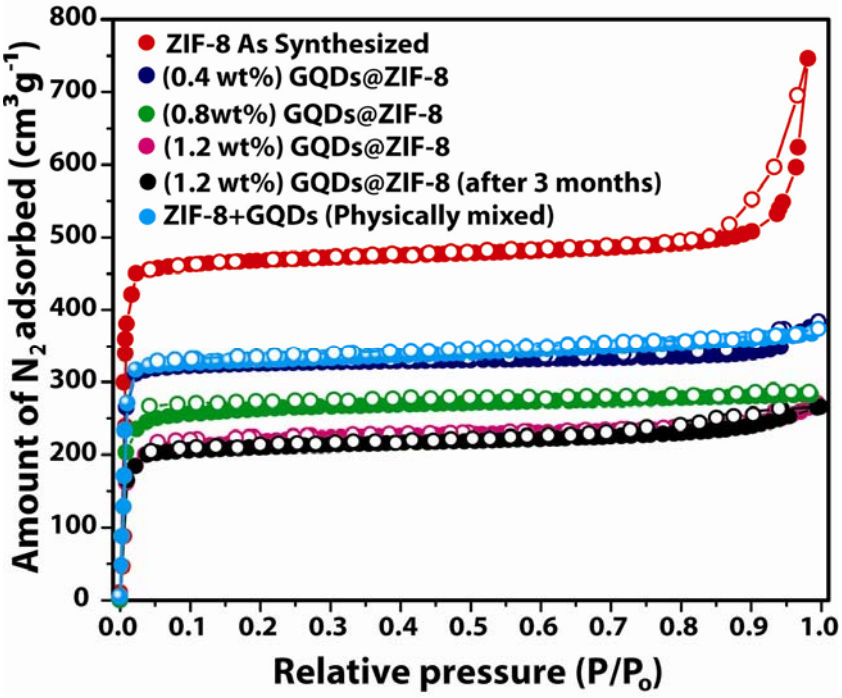

Fig. S6. The N_2 gas-sorption isotherms for as-synthesized ZIF-8 and (0.4 wt%) GQDs@ZIF-8, (0.8 wt%) GQDs@ZIF-8, (1.2 wt%) GQDs@ZIF-8, (1.2 wt%) GQDs@ZIF-8 composites (after 3 months of synthesis) and ZIF-8+GQDs (physically mixed) sample measured at 77 K. The filled and open circle represents adsorption and desorption branches, respectively.

Section 8: UV-Vis and PL spectra of all GQDs, ZIF-8 and composites:

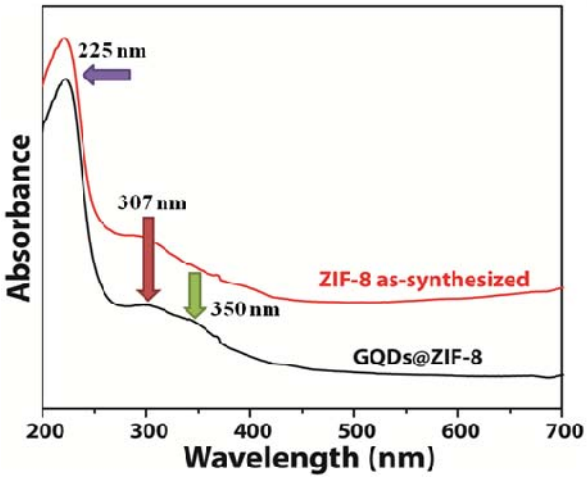

Fig. S7: Comparision of solid-state UV-DR spectra of ZIF-8 and GQDs@ZIF-8 composite.

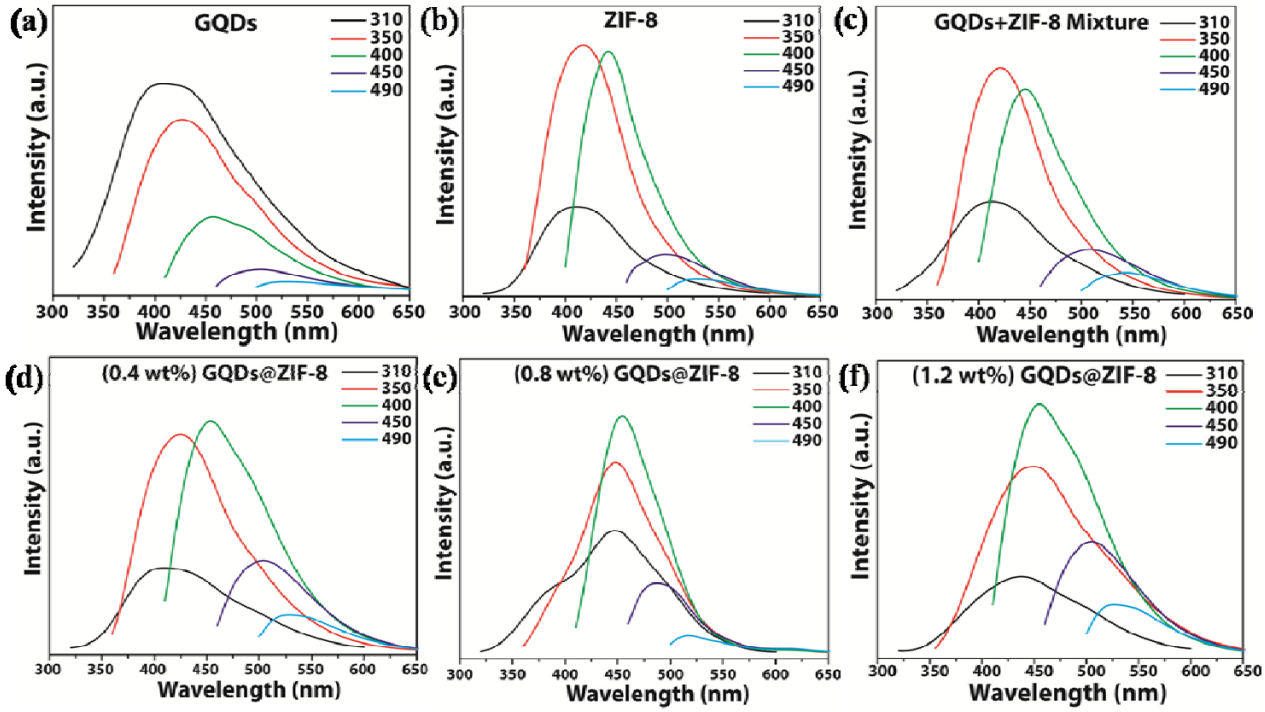

Fig. S8. Solid state PL spectra showing excitation dependant emission, of a) GQDs, b) ZIF-8, c) ZIF-8+GQDs (physically mixed), d) (0.4 wt%) GQDs@ZIF-8, e) (0.8 wt%) GQDs@ZIF-8, and f) (1.2 wt%) GQDs@ZIF-8 composites.

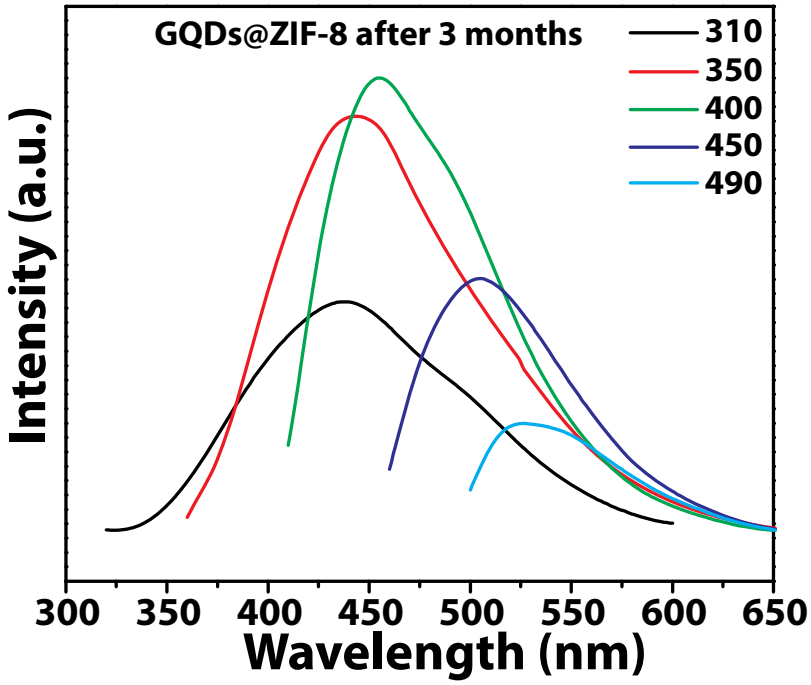

Fig. S9. Solid state PL spectra showing excitation dependent emission, of (1.2 wt%) GQDs@ZIF-8 composites after 3 months of synthesis.

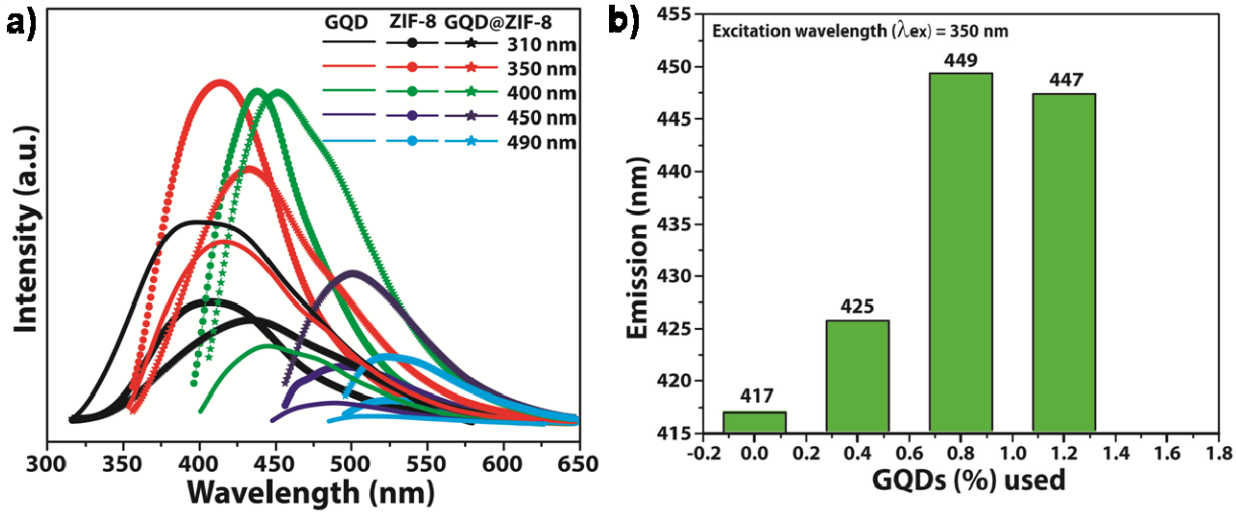

Fig. S10. a) Solid state PL spectra showing excitation dependant emission, of GQDs, ZIF-8 and GQDs@ZIF-8 composites at different excitation wavelength. b) Chart representing the comparison of fluorescence emission with different amount of GQDs used for the synthesis of GQDs@ZIF-8 composites.

Section 9: SEM and HR-TEM images:

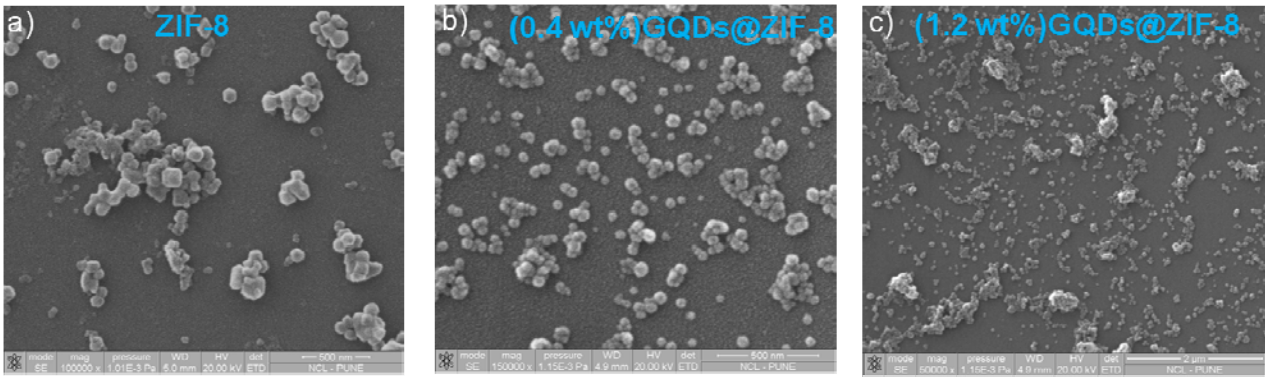

Fig. S11. SEM images of as-synthesized a) ZIF-8, b) (0.4 wt%) GQDs@ZIF-8 and c) (1.2 wt%) GQDs@ZIF-8 composites. [Figure 9b and 9c, are adopted from the main Draft (Figure 2b and 2c) to show the full scale bars and for better comparison between ZIF-8 and GQDs@ZIF-8 composites].

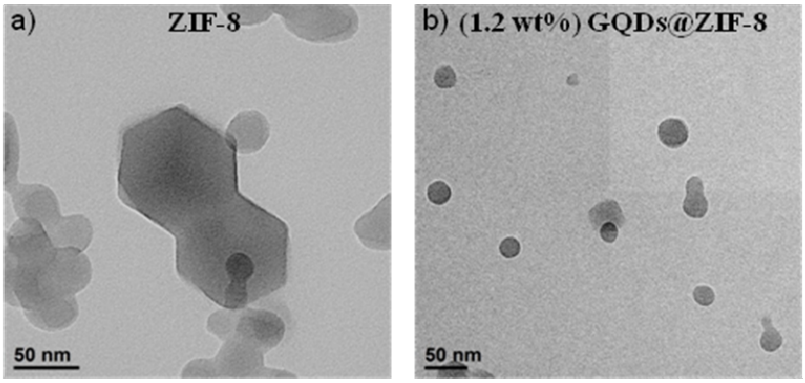

Fig. S12. HR-TEM images of as-synthesized a) ZIF-8 and b) (1.2 wt%) GQDs@ZIF-8 composites.

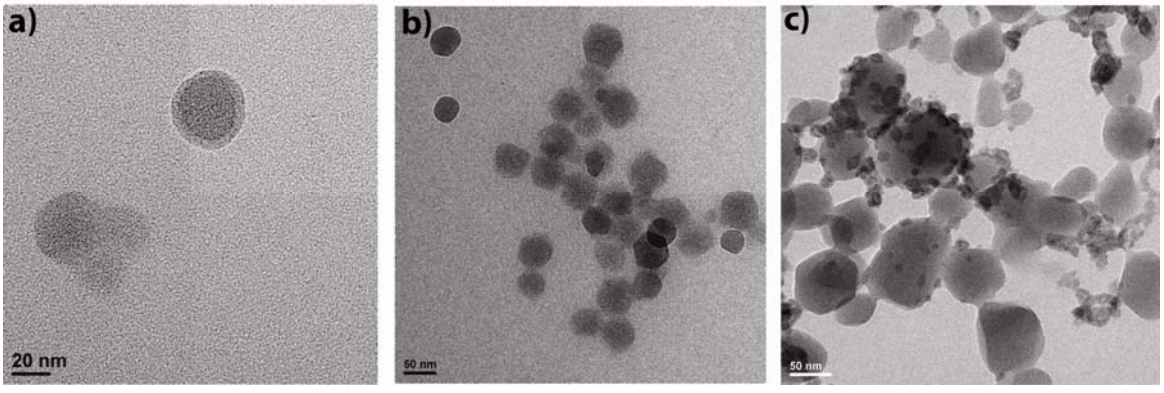

Fig. S13. HR-TEM images of products [(1.2 wt%) GQDs@ZIF-8 composites] obtained from reactions with different molar ratios of 2-methylimidazole (ligand) **:** zinc nitrate (metal) (a) 8:1 (b) 8:1.5 (c) 8:2.

From figure S13c) it is clear that for 8:2 (ligand to metal ratio) the GQDs are agglomerated out side the ZIF-8 crystals without encapsulating inside and hence the crystal morphology does not change much in this case as compared to the pristine ZIF-8.

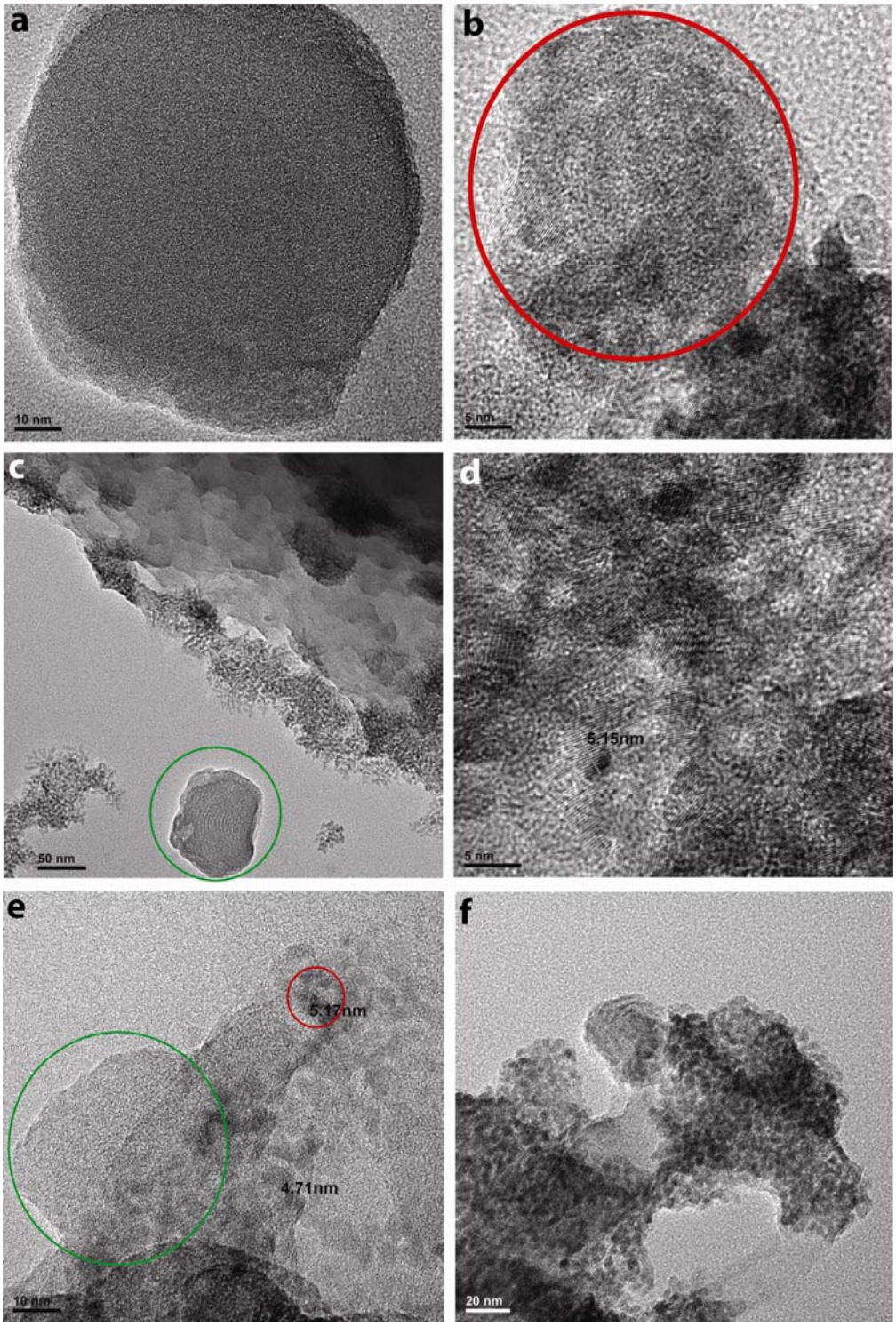

Fig. S14. HR-TEM images of GQDs@ZIF-8 composite after mechanical grinding using a mortar and pestle for 5 minutes, which shows that the ZIF-8 layers get delaminated and the GQDs are coming out from the trapped layers. (a) Spherical layers of ZIF-8, (b) Positions of GQDs after delamination of upper ZIF-8 layer (red circle), (c) Few ZIF-8 layers (green circle), (d) agglomeration of GQDs and one GQD (e) Partially delaminated ZIF-8 layer (green circle) and some suspended GQDs on the top of these layers (red circle).

Section 10: Confocal microscopy images:

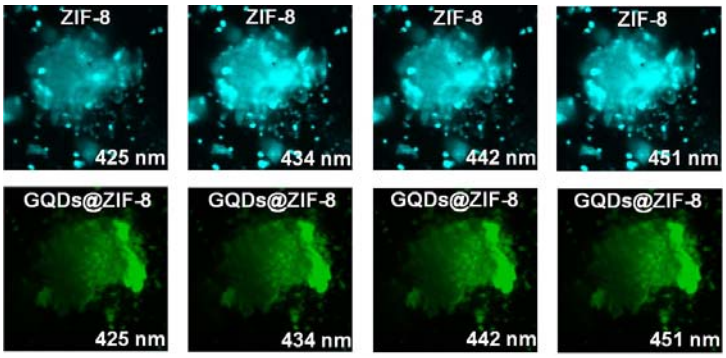

Fig. S15. Confocal images of ZIF-8 nanocrystals (cyan, top images) and (1.2 wt%) GQDs@ZIF-8 composites (false green colour given to the bottom images in order to clearly distinct from ZIF-8, above images), at excitation 405 nm. These images indicate that both ZIF-8 and GQDs@ZIF-8 composite gives emission in the range 425 nm to 451 nm.